

Precision Measurements of Reaction Wheel Disturbances with Frequency Compensation Process

Hwa-Suk Oh*, Dong-Ik Cheon

*School of Aerospace and Mechanical Engineering,
Hankuk Aviation University, Hwajun, Goyang 412-791, Korea*

The reaction wheel, an actuator for satellite attitude control, produces disturbance torque and force as well as axial control torque. The disturbances are so crucial to the pointing stability of this high precision satellite that a measurement of disturbances is necessary for such a satellite. The measurement table that is equipped with several load cells is one of the favorite types of measurement devices. The disturbance force and torque caused by the wheel's rotation, however, stimulate the elasticity of the loadcells from the measurement table and induce the vibration of the table. This then causes the measurement error, which is especially large near the resonance frequencies of the table. In order to reduce this type of error, a calibration process with frequency compensation is suggested in this paper. The "filtered" disturbance spectrum is obtained from the raw data and the degradation of data accuracy caused by the table vibration is alleviated. Since the exact measurement is made possible by this compensation process even in the resonance area, the measurement range can be expanded up to the frequency area including the resonance frequencies. The compensation method has been adopted for the HAU measurement table where three uni-directional loadcells are used. The validity of the use of uni-directional loadcells is also tested theoretically.

Key Words : Reaction Wheel, Torque Disturbance, Frequency Compensation, Measurement Table

1. Introduction

The reaction wheel is a kind of momentum exchange device and is widely used for spacecraft attitude control. (Vadali and Junkins, 1984 ; Sidi, 1997 ; Chen et al., 1999) By changing its speed, "axial" reaction torque is generated and used for attitude stabilization and control. The wheel, however, produces a disturbance torque and force also as by-products. The effects of wheel disturbances on the satellite's attitude error and stability are so critical that the influence of disturbances on the

quality of the attitude control should be analyzed prior to the application of the wheels on the satellite. To predict the effects of the disturbances on the spacecraft stability, mathematical models of disturbances have been studied and generated. (Bosgra and Prins, 1982 ; De Weck, 1998 ; Neat et al., 1998 ; Masterson et al., 1999, 2002) Since reaction wheels are operated at a range of speeds on satellites, they generate disturbances on a wide spectrum. The variety of spectrum should thus be reflected on the mathematical model of the disturbance. A stochastic broad-band model based on the discrete frequency model was created to predict the power spectral density. (Neat et al., 1998) An analytical model was developed using an energy method, which included the effects of the wheel structural flexibility. An experimental modeling methodology combined with a MATLAB tool box was developed for Hubble Space Tele-

* Corresponding Author,
E-mail : hsoh@hau.ac.kr
TEL : +82-2-300-0284; FAX : +82-2-300-0284
School of Aerospace and Mechanical Engineering,
Hankuk Aviation University, Hwajun, Goyang 412-791, Korea. (Manuscript Received July 23, 2004;
Revised November 6, 2004)

scope. (Masterson et al., 2002) The empirical model is represented in either the time domain or the frequency domain.

The stability analysis depends heavily on the quality of the disturbance model, whose parameters are determined from the disturbance spectrum on each wheel speed. The disturbance measurements are performed with several kinds of devices. The measurement table supported by a set of loadcells is one of the favorite devices for the disturbance measurement. (Bosgra and Prins, 1982; De Weck, 1998; Neat et al., 1998; Masterson et al., 1999, 2002; Oh et al., 2001) While the test reaction wheel rotates on the measurement table, the disturbance force and torque are determined from the combination of the deflection signals from the supporting loadcells. The disturbance, however, stimulates the elasticity of the supporting loadcells and induces the vibration of the table. The vibration results in the amplification of the disturbance signal. The amplification degrades the measurement accuracy especially around the resonance frequencies of the corresponding structure modes. In this paper, we want to introduce a methodology to reduce this type of measurement error. One of the other causes of the disturbance amplification is the structural flexibility in the wheel, (Masterson et al., 2002) which is not treated in this paper.

In order to avoid the large measurement errors near resonance frequencies, a number of different measurements are commonly performed in the range of much lower frequencies than the resonance frequencies. As a result, the measurement frequency range becomes narrower. Even inside the non-resonance measurement range, however, there still exist measurement errors due to the vibration of the table. This type of error has been considered inevitable and neglected so far in the conventional measurement method. For the purpose of overcoming this defect, a calibration method based on the acceleration compensation on the time domain was suggested. (Oh et al., 2001) But, the method was found to be inadequate for the analysis of frequency characteristics of disturbances. Frequency spectral data is usually preferred for the analysis of the frequency

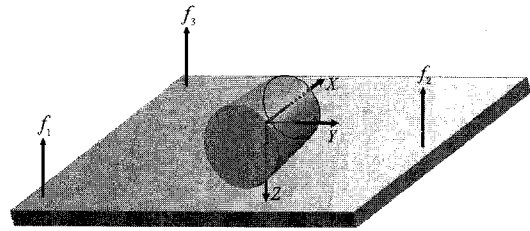


Fig. 1 Schematic of HAU disturbance measurement table

characteristics of data. (Kim et al., 1996) A new compensation method on the frequency domain is thus proposed in this paper.

By post-calibrating the raw measurement data in the frequency domain, the “filtered” disturbance spectrums are obtained and the data accuracy degradation caused by the vibration of the measurement table is alleviated. Measurement data then becomes reliable even at the resonance frequencies of the table. The measurement frequency range could thus be expanded to the area of far higher frequencies than that of the resonance ones.

Another contribution of this paper is the adoption of uni-directional loadcells for the measurement of three-dimensional torque and force disturbances. Conventional disturbance measurement tables usually adopt three-directional loadcells. However, it is shown in this paper that uni-directional loadcells can also be used for measuring the three dimensional disturbance torques and forces. The validity of the use of the uni-directional loadcells is verified for the measurement table made in the SatCon laboratory in Hankuk Aviation University. (Oh et al., 2001; Seo, 2002; Cheon, 2002) The table is composed of a rigid plate supported on three uni-directional loadcells and the data acquisition board. The test reaction wheel is the Development Model wheel for Korean Scientific Satellite-I. (Oh et al., 2001) The test configuration of the reaction wheel on the measurements table is depicted in Fig. 1.

2. Disturbance Model of Reaction Wheel

Wheel disturbances are caused by various kinds

of sources : flywheel imbalance, bearing irregularity, motor disturbances, motor driver errors, and the internal structural compliance, etc. Force and torque disturbances can be classified by the frequency characteristics. These are the disturbances proportional to the harmonics of the wheel speed and the disturbances that are independent of wheel speed. Speed-dependent force and torque disturbance can be modeled experimentally as follows : (De Weck, 1998 ; Bosgra and Prins, 1982 ; Masterson et al., 2002)

$$F(t) = \sum F_i \Omega^2 \sin(2\pi h_i \Omega t + \alpha_i), \quad (1)$$

$$T(t) = \sum T_i \Omega^2 \sin(2\pi h_i \Omega t + \alpha_i), \quad (2)$$

where $F(t)$ and $T(t)$ are the disturbance force and torque, respectively, F_i and T_i the amplitude coefficients of the i -th harmonic, Ω the wheel speed, h_i the i -th harmonic number (or order), and α_i the phase angle. An internal structural compliance induces the axial and radial translation vibration mode, in which the frequency-dependent disturbances occur. The rocking mode, another internal compliance mode, behaves differently than the translational mode. It is a function of the wheel speed and splits into two natural frequencies forming a V shaped ridge in the waterfall diagram. The splitting is known due to the gyroscopic effects of the spinning wheel. (Masterson et al., 1999)

When the disturbance models are assumed as above, it is necessary to determine the magnitude coefficients F_i and T_i . The validity of the model depends on the accuracy of the coefficients. The coefficients are decided empirically from the vibration test data. That is, the test reaction wheel is run on specific speeds on the measurement table and the disturbances are determined from the combinations of the deflection signals from the loadcells of the measurement table.

3. Disturbance Measurement Principle with Uni-directional LoadCells

Since conventional disturbance measurement tables usually adopt three-directional loadcells, we first derive the dynamic equations of a mea-

surement table that is equipped with three-directional loadcells. However, because we used the lab-made measurement table that is equipped with the unidirectional loadcells, the feasibility analysis of the uni-directional loadcell table is thus followed.

In the case of the three-directional loadcells, they can be modeled as three-directional springs and dampers attached at the supporting points as shown in Fig. 2. The measurement table is then modeled as one rigid plate that is supported by several linear springs and dampers.

Equations of translational motion of the table can be written as :

$$F_x + \sum_i f_{x_i} = m \Delta \ddot{x}_c, \quad (3)$$

$$F_y + \sum_i f_{y_i} = m \Delta \ddot{y}_c, \quad (4)$$

$$F_z + \sum_i f_{z_i} = m \Delta \ddot{z}_c, \quad (5)$$

where F_x , F_y , F_z are the disturbance forces of reaction wheel, f_{x_i} , f_{y_i} , f_{z_i} the supporting forces of the i -th loadcell, m the total mass of the wheel-table combined system (hereafter, the table system) and Δx_c , Δy_c , Δz_c the translational displacements of the center of mass (x_c , y_c , z_c) of the table system. The reference point "o" is the origin of the inertial frame. The supporting forces f_{x_i} , f_{y_i} , and f_{z_i} are due to the elastic deflection and the viscous friction of the i -th loadcell as follows :

$$f_{x_i} = -k_x \Delta x_i - c_x \Delta \dot{x}_i, \quad (6)$$

$$f_{y_i} = -k_y \Delta y_i - c_y \Delta \dot{y}_i, \quad (7)$$

$$f_{z_i} = -k_z \Delta z_i - c_z \Delta \dot{z}_i, \quad (8)$$

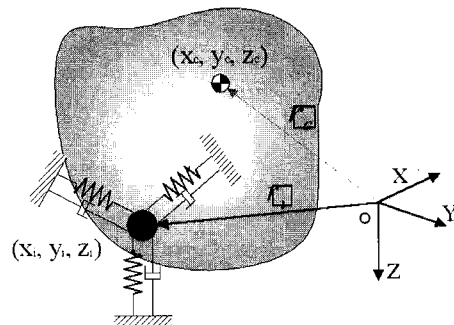


Fig. 2 Dynamic model of disturbance measurement table

where k is the loadcell spring constant, c the damping coefficient, and $\Delta x_i, \Delta y_i, \Delta z_i$ the deflections of the i -th loadcell. The displacements of each loadcell can be written as

$$\Delta x_i = \Delta x_c + z_i \theta_y - y_i \theta_z, \quad (9)$$

$$\Delta y_i = \Delta y_c - z_i \theta_y + x_i \theta_z, \quad (10)$$

$$\Delta z_i = \Delta z_c + y_i \theta_x - x_i \theta_y, \quad (11)$$

where $\theta_x, \theta_y, \theta_z$ are the rotational displacements of the table system, and x_i, y_i, z_i the position coordinates of the i -th loadcell from the reference point "o".

In the case of the rotation angles are assumed to be small, the rotational equations of motion are decoupled with each other as follows :

$$T_x + \sum_i f_{z_i} y_i - \sum_i f_{y_i} z_i = J_x \ddot{\theta}_x, \quad (12)$$

$$T_y - \sum_i f_{z_i} x_i + \sum_i f_{x_i} z_i = J_y \ddot{\theta}_y, \quad (13)$$

$$T_z - \sum_i f_{x_i} y_i + \sum_i f_{y_i} x_i = J_z \ddot{\theta}_z, \quad (14)$$

where T_x, T_y, T_z are the disturbance torques of the reaction wheel and J_x, J_y, J_z are the moments of inertia of the table system.

In the conventional measurement methods, the dynamic effects of the table are ignored. The disturbance forces and torques are then determined by measuring only $f_{x_i}, f_{y_i}, f_{z_i}$ as follows :

$$F_x = - \sum_i f_{x_i}, \quad (15)$$

$$F_y = - \sum_i f_{y_i}, \quad (16)$$

$$F_z = - \sum_i f_{z_i}, \quad (17)$$

$$T_x = - \sum_i f_{z_i} y_i + \sum_i f_{y_i} z_i, \quad (18)$$

$$T_y = \sum_i f_{z_i} x_i - \sum_i f_{x_i} z_i, \quad (19)$$

$$T_z = \sum_i f_{x_i} y_i - \sum_i f_{y_i} x_i, \quad (20)$$

where the loadcell forces are measured statically as

$$f_{x_i} = -k_x \Delta x_i, \quad (21)$$

$$f_{y_i} = -k_y \Delta y_i, \quad (22)$$

$$f_{z_i} = -k_z \Delta z_i. \quad (23)$$

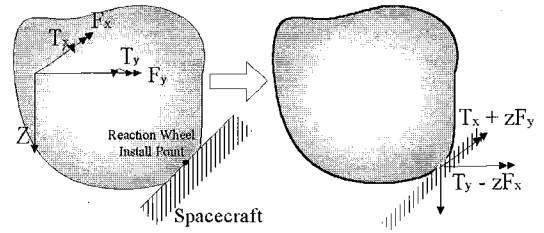


Fig. 3 Equivalent torque disturbances acting on satellite supporting point

If $z_i \equiv z$, i.e., when the supporting levels of all loadcells are equal, we can measure the "equivalent torques" as $T_x' \equiv T_x + zF_y$ and $T_y' \equiv T_y - zF_x$, which are the actual net torques of the reaction wheel exerted on the supporting point in the x and y direction. Equations (17) ~ (19) can then be rewritten as

$$F_z = - \sum_i f_{z_i}. \quad (24)$$

$$T_x' = - \sum_i f_{z_i} y_i. \quad (25)$$

$$T_y' = - \sum_i f_{z_i} x_i. \quad (26)$$

Therefore, as long as loadcells are located on the same level, it is sufficient to measure the z directional load f_{z_i} for the measurements of the x and y direction torques and the z direction force. That means that uni-directional load cell can be used for measuring torque disturbance in addition to force. (Oh, 2003)

4. Example Run Tests

The test reaction wheel is the Development Model for Korean Scientific Satellite-I. (Oh and Yoon et al., 2001) The wheel weighs approximately 1 kg with a maximum torque capacity of greater than 60 mNm. The design nominal operation speed is 1000 rpm. It operates either on the speed control mode or on the torque control mode. The configuration of the wheel is shown in Fig. 4.

In order to measure the force and torque disturbances of the reaction wheel with a uni-directional loadcell torque table, the wheel is run in speed control mode from 0 to 1000 rpm in equal increments of speed. While the loadcell signals are in acquisition, the disturbances are

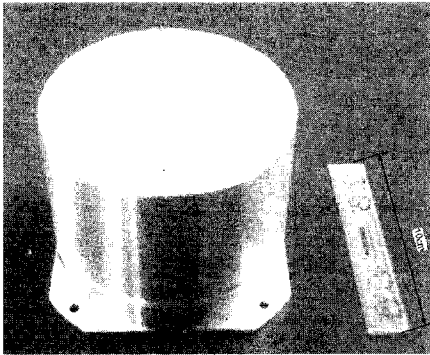
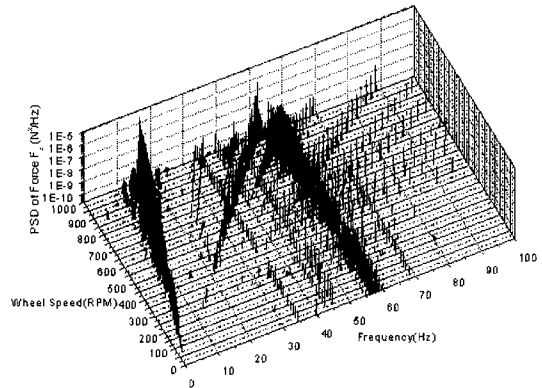


Fig. 4 Test reaction wheel-HAURW3

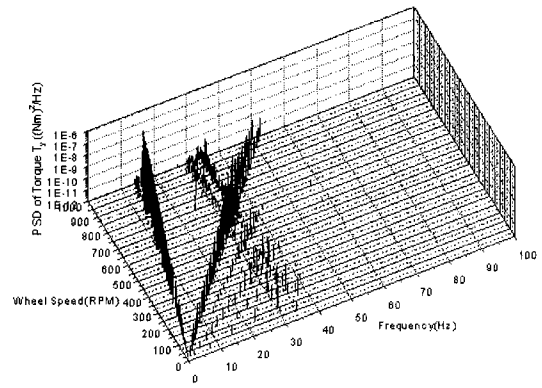
then determined by following the Eqs. (24) ~ (26). The time histories of the measured data are transformed to three-dimensional Power Spectral Density (PSD) diagrams which are known as waterfall plots. (Silva, 1999) These are seen as shown in Fig. 5. Note that in addition to the typical diagonal ridges, several spectral ridges are visible near 30Hz, 40Hz, and 60Hz, which are independent of the wheel speed. These ridges are found not due to the wheel disturbance itself but due to the resonance of the table, (Seo, 2002) which must induce the measurement errors. There exists no frequency independent disturbance other than the table resonance induced terms. In addition, the V-shaped ridge caused by the internal rocking mode is also not appeared.

5. Effects of Table Vibration

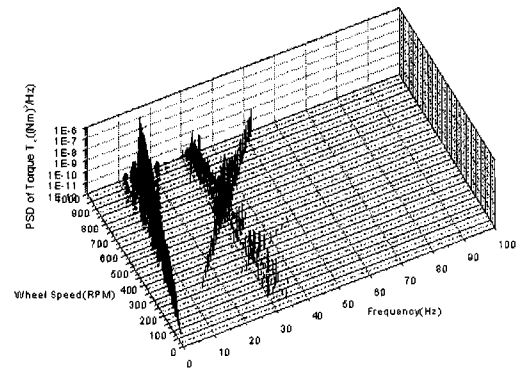
The above data is measured on the assumption of the static state. Figure 5 shows that the magnitudes of the wheel disturbances are so amplified near the table resonance frequencies that it will lead to a large amount of errors. To avoid these large errors near the resonance frequencies, conventional measurements are usually performed in the range of a much lower frequency than that of the resonance ones. However, if the resonance frequencies of the table system exist near the major disturbance frequencies, the errors are inevitable. In this case, a compensation process is required to cure this error and to get more reliable data. A compensation method in the frequency domain is suggested in this paper.



(a) F_z



(b) T_x'



(c) T_y'

Fig. 5 PSD of uncompensated disturbance data

Consider the equations of the motion of the table system shown in Eqs. (3) ~ (14). When the uni-directional loadcells are used in the measurement table, no deflection is assumed on the x or y direction. The forces F_x and F_y are then considered just as rigid as the constraint forces which can be represented as Eqs. (15) and (16).

However, since the motion is allowed in the z -direction, the z directional force F_z in Eq. (5) can be re-written using Eqs. (8) and (11) as

$$F_z = \sum_i \{ k_z (\Delta z_c + y_i \theta_x - x_i \theta_y) + c_z (\Delta \dot{z}_c + y_i \dot{\theta}_y - x_i \dot{\theta}_x) \} + m \Delta \ddot{z}_c \quad (27)$$

Disturbance torque equations (12) and (13) can then be re-arranged on the assumption $z_i \equiv z$ as

$$T_x + z F_y = J_x \ddot{\theta}_x - \sum_i f_{z_i} y_i, \quad (28)$$

$$T_y - z F_x = J_y \ddot{\theta}_y + \sum_i f_{z_i} x_i. \quad (29)$$

Furthermore, if the loadcells are located symmetrically as $\sum y_i \theta_x = 0$ and $\sum x_i \theta_y = 0$ about x -axis (Fig. 1 is such a case), then the force disturbance F_z , and the equivalent torques T_x' and T_y' can be simplified as

$$F_z = m \Delta \ddot{z}_c + \sum c_z \Delta \dot{z}_c + \sum k_z \Delta z_c, \quad (30)$$

$$T_x' = J_x \ddot{\theta}_x + \sum_i c_z y_i^2 \dot{\theta}_x + \sum_i k_z y_i^2 \theta_x, \quad (31)$$

$$T_y' = J_y \ddot{\theta}_y + \sum_i c_z x_i^2 \dot{\theta}_y + \sum_i k_z x_i^2 \theta_y. \quad (32)$$

Finally, the equations for F_z , T_x' , and T_y' can be written as

$$F_z = M_z \Delta \ddot{z}_c + C_z \Delta \dot{z}_c + K_z \Delta z_c, \quad (33)$$

$$T_x' = J_x \ddot{\theta}_x + C_x \dot{\theta}_x + K_x \theta_x, \quad (34)$$

$$T_y' = J_y \ddot{\theta}_y + C_y \dot{\theta}_y + K_y \theta_y, \quad (35)$$

where $M_z \equiv m$, $C_z \equiv \sum c_z$, $K_z \equiv \sum k_z$, $C_x \equiv \sum c_z y_i^2$, $C_y \equiv \sum c_z x_i^2$, $K_x \equiv \sum k_z y_i^2$, and $K_y \equiv \sum k_z x_i^2$. With the assumptions of small deflections and no transverse translational motion, three equations have become completely decoupled as above. Thus we can take compensation easily and independently.

In the conventional static measurements, the dynamic effects of the table have been neglected. That is, the acceleration and velocity terms in Eqs. (33) ~ (35), are neglected and only stiffness terms are reflected on the measurements as

$$F_z = K_z \Delta z_c, \quad (36)$$

$$T_x' = K_x \theta_x, \quad (37)$$

$$T_y' = K_y \theta_y, \quad (38)$$

Then the neglected terms ($M_z \Delta \ddot{z}_c + C_z \Delta \dot{z}_c$), ($J_x \ddot{\theta}_x + C_x \dot{\theta}_x$), ($J_y \ddot{\theta}_y + C_y \dot{\theta}_y$) contribute to the measurement errors. On the contrary, if the dynamic terms of Δz_c , θ_x , and θ_y motions are included as in Eqs. (33) ~ (35), more reliable data of disturbances F_z , T_x' , and T_y' can be obtained. It can be performed either in the time-domain (Oh and Lim et al., 2001) or in the frequency domain. (Seo, 2002; Cheon, 2002) In this paper, the frequency domain analysis method is applied to get the information in frequency characteristics.

6. Vibration Compensation Process in the Frequency Domain

Since only the displacements Δz_c , θ_x , and θ_y are measured on tests, in order to get the exact data F_z , T_x' , and T_y' as in Eqs. (33) ~ (35), we need the acceleration and the velocity information. They can be obtained by some post-process in frequency domain rather than the direct measurement of them in real time. Taking Fourier transforms of Eqs. (33) ~ (35) results into

$$F_z(\omega) = [(-M_z \omega^2 + K_z) + j(C_z \omega)] \Delta Z_c(\omega), \quad (39)$$

$$T_x(\omega) = [(-I_x \omega^2 + K_x) + j(C_x \omega)] \theta_x(\omega), \quad (40)$$

$$T_y(\omega) = [(-I_y \omega^2 + K_y) + j(C_y \omega)] \theta_y(\omega), \quad (41)$$

Products by their conjugates lead to power spectral densities as

$$S_{F_z}(\omega) = [(-M_z \omega^2 + K_z)^2 + (C_z \omega)^2] S_{\Delta z_c}(\omega), \quad (42)$$

$$S_{T_x}(\omega) = [(-I_x \omega^2 + K_x)^2 + (C_x \omega)^2] S_{\theta_x}(\omega), \quad (43)$$

$$S_{T_y}(\omega) = [(-I_y \omega^2 + K_y)^2 + (C_y \omega)^2] S_{\theta_y}(\omega), \quad (44)$$

where $S_i(\omega)$ is the power spectral density of the i -th variable. That is, the compensated spectra of F_z , T_x' and T_y' can be obtained by post-processing the displacement spectra of $\Delta Z_c(\omega)$,

$\theta_x(\omega)$, and $\theta_y(\omega)$ in ω -space as in Eqs. (42) ~ (44). The displacements Δz_c , θ_x , and θ_y are obtained from the deflections of loadcells as

$$\begin{bmatrix} \Delta z_c \\ \theta_x \\ \theta_y \end{bmatrix} = A \begin{bmatrix} \Delta z_1 \\ \Delta z_2 \\ \dots \\ \Delta z_n \end{bmatrix} \quad (45)$$

where the matrix A represents the installation configuration matrix of loadcells. The magnitude coefficients of F_z , T_x' and T_y' are derived from the power spectra shown in Eqs. (42) ~ (44). This procedure is the base idea of the frequency compensation process.

The precision of the compensation process depends on how exactly the table vibration is modeled and how accurately the model parameters are determined in Eqs(33) ~ (35). The parameters of the table system have been determined through the impact tests in this study. Figure 6 shows the results of the compensated spectra of F_z , T_x' and T_y' . The peaks due to the resonance of the measurement table (near $30H_z$, $40H_z$ and $60H_z$ shown in Fig. 5) have almost been removed and the more accurate disturbance data has been successfully obtained. The compensated data could be used for the determination of precision disturbance models, e.g., for Eqs. (1) and (2). Discussions on the coefficient determination procedure from the compensated data and on the procedure of the extraction and the validation of the wheel model are beyond the scope of this paper. A coefficient extraction procedure is introduced in reference 10, for example.

7. Conclusions

Torque and force disturbances of the wheel have been measured with the measurement table equipped with the uni-directional loadcells. Adaptability of the uni-directional loadcells on the measurement table has then been verified theoretically. The suggested frequency compensation method has been found to compensate the vibration of the measurements table well. This had then caused the measurement errors, especially near the resonance frequencies. Disturbance amplification due to the vibration of the measurement table near the resonance frequencies has been efficiently removed by post-processing the measurement data. The errors due to the table vibration have been successfully reduced. The suggested frequency compensation method shown in this paper can expand the measurement range wider, up to the area including the resonance

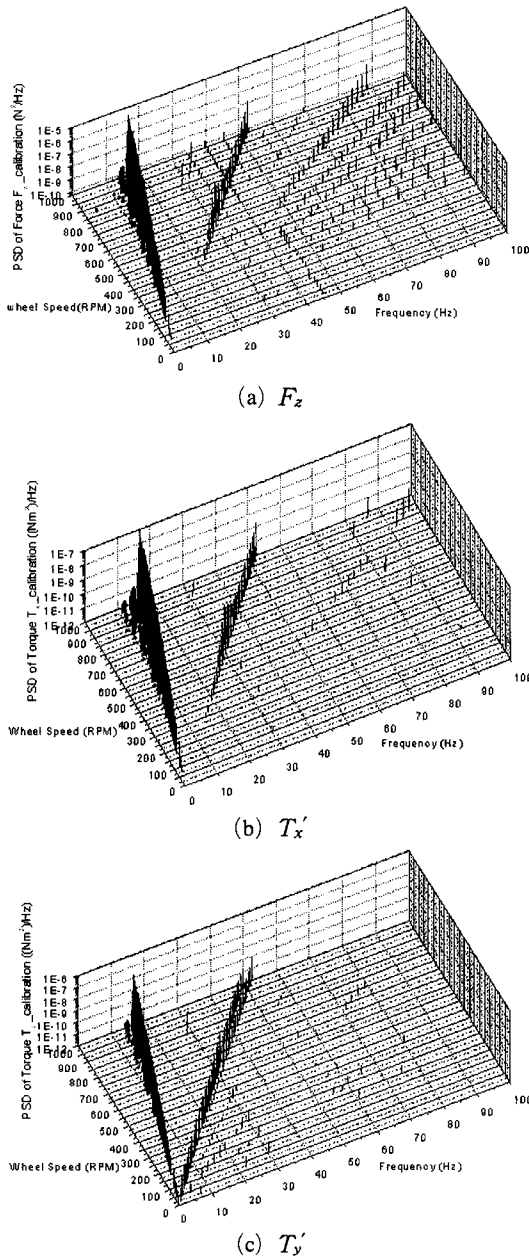


Fig. 6 PSD of compensated disturbance data

frequencies. With a slight modification of this compensation method, the idea of this method can then be expanded to the full three-dimensional compensation process.

References

- Bosgra, J. A., and Prins, J. M., 1982, "Testing and Investigations of Reaction Wheels," *IFAC Automatic Control in Space*, Noordwijkerhout, The Netherlands.
- Chen, X., Steyn, W. H., Hodgart, S. and Hashida, Y., 1999, "Optimal Combined Reaction-Wheel Momentum Management for Earth-Pointing Satellites," *Journal of Guidance, Control, and Dynamics*, Vol. 22, No. 4, pp. 542~550.
- Cheon, D. I., 2002, "Experimental Modeling of Reaction Wheel Disturbances and Effects on the Attitude of Satellites," Thesis, Hankuk Aviation University, Korea.
- De Weck, O., 1998, "Reaction Wheel Disturbance Analysis," MIT-SSL-NGST-98-1, MIT, MA.
- Kim, J. Y., Yoon, E. J., Chang, S. J., Kim, D. Y. and Jeong, W. B., 1996, "A Study on the Determination of Optimal Reference Spectrum for Random Vibration Control in Environmental Vibration Test," *KSME International Journal*, Vol. 10, No. 2.
- Masterson, R., Miller, D. and Grogan, R., 1999, "Development of Empirical and Analytical Reaction Wheel Disturbance Models," AIAA paper A99-24904, Missouri.
- Masterson, R., Miller, D. W. and Grogan, R., 2002, "Development and Validation of Reaction Wheel Disturbance Models: Empirical Model," *Journal of Sound and Vibration*, Vol. 249, No. 3, pp. 575~598.
- Neat, G. W., Melody, J. W. and Lurie, B. J., 1998, "Vibration Attenuation Approach for Spaceborne Optical Interferometers," *IEEE Transaction on Control Systems Technology*, Vol. 6, pp. 689~700.
- Oh, H. S., 2003, "Method and Apparatus for Measuring with One-Dimensional Loadcell the Dynamic Torque of High-Speed Rotary Machine," *Patent No. 0375628*, Korea.
- Oh, H. S., Kwon, J. W., Lee, H. Y., Nam, M. R. and Park, D. J., 2001, "Torque and Force Measurement of a Prototype HAU Reaction Wheel and the Effects of Disturbance on the Attitude Stability of Spacecraft," *KSME International Journal*, Vol. 15, No. 6, pp. 743~751.
- Oh, H. S., Lim, Y. S., Seo, Y. K., Jang, Y. G., Hwang, J. H., Park, Y. C., Lee, H. U., Nam, M. R. and Park, D. J., 2001, "Measurements of Reaction Wheel Torque Minimizing the Effects of the Vibration of the Torque Measuring Scale," *KSAS Fall Annual Meeting*, Korea.
- Oh, H. S., Yoon, Y. D., Kwon, J. W., Choi, S. W., Choi, S. C., Lee, B. U., Lim, Y. S., Cheon, D. I. and Seo, Y. K., 2001, "Development of an Attitude Control Actuator System for Small Satellite," Ministry of Science and Technology, Korea.
- Seo, Y. K., 2002, "Precise Measurement and Parameter Identification of the Disturbances of Satellite Reaction Wheel Calibrating the Vibration of Torque Measuring Table," Thesis, Hankuk Aviation University, Korea.
- Sidi, M. J., 1997, *Spacecraft Dynamics and Control*, Cambridge University Press, pp. 160~185.
- Silva, C. W., 1999, *Vibration*, CRS Press, New York, NY, pp. 186~189.
- Vadali, S. R. and Junkins, J. L., 1984, "Optimal Open-Loop and Stable Feedback Control of Rigid Spacecraft Attitude Maneuvers," *The Journal of the Astronautical Sciences*, Vol. 32, No. 2, pp. 105~122.